Investigation of a Non-alcoholic Fatty Liver Disease Model Using ^{23}Na, ^{1}H and ^{31}P MR Techniques

P. Hopewell[1,2], and N. Bansal[1]

[1]Department of Radiology, Indiana University, Indianapolis, IN, United States, [2]Weldon School of Biomedical Engineering, Purdue University, West Lafayette, IN, United States

Introduction

Non-alcoholic fatty liver disease (NAFLD), a component of the metabolic syndrome shown to lead to cirrhosis and cancer, has reached epidemic proportions in the developed world. Since the current diagnosic standard requires liver biopsy, noninvasive detection of a marker representing the transition from simple steatosis to steatohepatitis is in dire need. One possible marker for this transition is the detection of an altered transmembrane sodium gradient, a crucial part of normal hepatocellular function that has been known to be disrupted in various disease states. The current study evaluated the ability of single quantum (SQ) and triple quantum-filtered (TQF) ^{23}Na MRI techniques to monitor the progression of liver injury in a murine model of NAFLD, rats fed a methionine- and choline-deficient diet (MCDD), a treatment that increases hepatic fat content by promoting peripheral lipolysis and hepatic uptake of fatty acids. Additional ^{1}H MRI/S studies were performed to assess the amount and type of hepatic lipid accumulation. In addition, the mechanisms behind the changes in SQ and TQF ^{23}Na MRI were examined using shift reagent (SR)-aided ^{23}Na and ^{31}P MRS techniques.

Methods

Wistar rats (~250 g) were placed on MCDD after baseline SQ and MQF ^{23}Na MRI and ^{1}H MRI/S were collected. Additional data were collected at 2, 5, and either 10 weeks or 15 weeks after initiating MCDD treatment. MR data were acquired with a Varian 9.4 Tesla horizontal bore system. A 63-mm birdcage quadrature coil tuned to 400 MHz was used to collect all ^{1}H MRI/S data. Trans-axial images were collected using a spin-echo multislice sequence. Three total scans were performed: CHESS suppression applied at 4.7 ppm (H_2O), CHESS suppression at 1.3 ppm $(CH_2)_n$, and without frequency suppression. The following imaging parameters were used: 1 s repetition time (TR), 11 ms echo time (TE) and 2 min imaging time. Fat-to-water ratios were determined from the signal intensity (SI) observed in the region of interest (ROI) corresponding to liver only. Spectroscopy data was collected using a localized adiabatic selective refocusing (LASER) sequence and respiratory gating. The spin-echo image without suppression was used as a scout image for voxel placement. The following imaging parameters were used: TR = 1 s, TE = 37.6 ms, 8 μL^3 voxel size and 2 min total collection time. 3D SQ trans-axial ^{23}Na MRI were obtained with a home-built loop-gap resonator tuned to 106 MHz. The SQ ^{23}Na MRI were collected using a gradient-echo (GE) imaging sequence and following imaging parameters: TR = 50 ms, TE = 4.5 ms and 10 min total imaging time. TQF ^{23}Na MRI employed the same parameters as used for SQ ^{23}Na MRI except TR = 100 ms and 50 min total imaging time. SR-aided ^{23}Na and ^{31}P MRS experiments were performed after the MRI experiments to measure the relative intra- and extracellular spaces (rICS and rECS, respectively) and intra- and extracellular Na^+ concentrations ($[Na_i^+]$ and $[Na_e^+]$, respectively). Rats were surgically prepared for infusion of $TmDOTP^{5-}$ through the external jugular vein. A 2 cm diameter surface coil tunable to 106 MHz for ^{23}Na and 163 MHz ^{31}P spectra was placed over the exposed liver. Histologic samples were fixed in formalin and stained with H&E and trichrome stains.

Results

Fat-to-water SI (8.2±0.78) from ^{1}H MRI peaked at week 2. The signal area ratios calculated from ^{1}H LASER MRS peaked as follows ($p<0.02$): $(CH_2)_n/H_2O$ at week 5 (7.3±0.38), CH_2/CH_3 at week 2 (12.4±3.1), and unsaturated fatty acids/CH_2 at 10 weeks (0.23±0.014). Figures 1 and 2 are examples of water- and fat-suppressed ^{1}H MRI and ^{1}H MRS at baseline and 2 weeks after initiating MCDD. SQ and TQF ^{23}Na SI (Figure 3) decreased

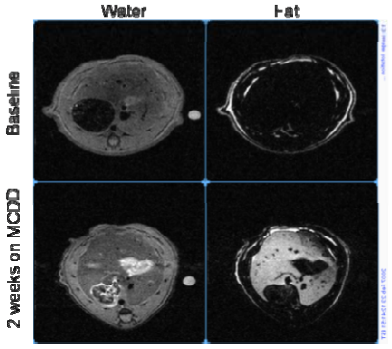

Fig 1: Selected sections from transaxial ^{1}H water (left) and fat (right) MRI of rat liver before (top) and 2 weeks (bottom) after initiating MCD diet

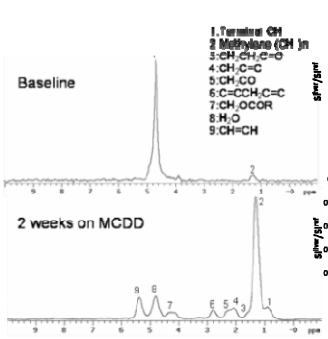

Fig. 2: Localized ^{1}H spectra of rat liver before and 2 weeks after initiating MCD diet.

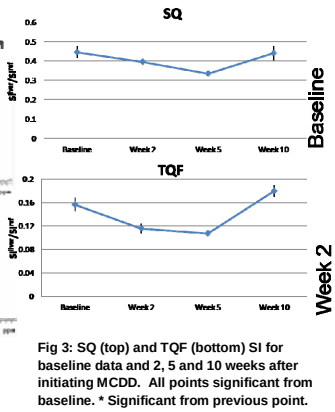

Fig 3: SQ (top) and TQF (bottom) SI for baseline data and 2, 5 and 10 weeks after initiating MCDD. All points significant from baseline. * Significant from previous point.

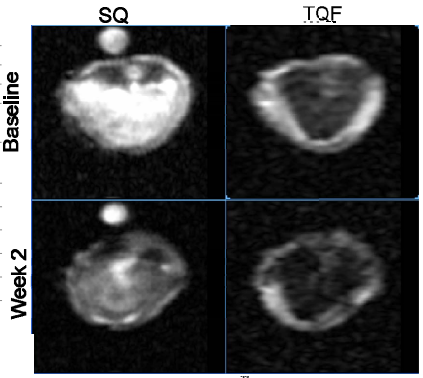

Fig 4: SQ (left) and TQF (right) ^{23}Na MRI of liver for baseline (top) and 2 weeks after initiating MCDD (bottom).

by week 5 and increased at week 10 to values significant from week 5 ($p<0.02$). Figure 4 shows representative SQ and TQF ^{23}Na MRI at baseline and 2 weeks post-MCDD treatment. Histological data showed increased lipid content at week 2, fibrosis development at week 10 and advanced fibrosis at week 15. Initial SR data (Figure 5) showed a trend of increasing $[Na^+]_i$, yet the only significant data was an increase in dry weight at week 15.

Discussion and Conclusions

The decrease in SQ and TQF ^{23}Na MRI SI at week 2 and 5 is hypothesized to be due to Na^+'s insolubility in lipid, leading to a relative decreased concentration. Similarly, lipid content decreased and ^{23}Na MRI SI increased by week 10. However, alternative theories for the increased TQF SI at week 10 include: 1) increased fibrosis-associated macromolecule deposition in the extracellular space and 2) increased $[Na^+]_i$ due to ATP depletion, both of which causing an increase in TQF ^{23}Na SI. Preliminary histological data and SR data support both explanations.

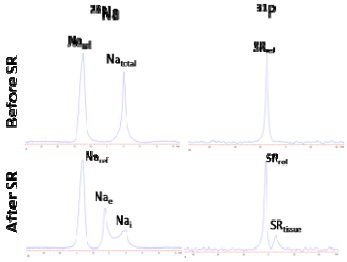

Fig. 5: ^{23}Na spectra (left) and ^{31}P spectra (right) before (top) and after (bottom) SR injection.

Even though water- and fat-suppressed MRI did not directly correlate temporally with the dominant lipid peak, $(CH_2)_n$, the changes in other lipid peaks showed that steatosis to fibrosis progression is not merely a change in $(CH_2)_n/H_2O$, but changes in different lipid moieties. Selective frequency suppression/excitation techniques are acceptable when suppression or excitation pulse bandwidths do not interfere with the frequency of neighboring peaks in the Fourier domain. Yet when peaks of interest are near or within the suppression/excitation frequency (e.g., the unsaturated fatty acid peak at 5.3 ppm during H_2O suppression), signal loss from non-H_2O moieties. In conclusion, histological data correlates with ^{1}H and SQ and TQF ^{23}Na MRI/S, prompting further development for NAFLD diagnosis and staging.